

## *CheShift-2* resolves a local inconsistency between two X-ray crystal structures

Jorge A. Vila · Shih-Che Sue · James S. Fraser ·  
Harold A. Scheraga · H. Jane Dyson

Received: 6 July 2012 / Accepted: 17 August 2012  
© Springer Science+Business Media B.V. 2012

**Abstract** Since chemical shifts provide important and relatively accessible information about protein structure in solution, a Web server, *CheShift-2*, was developed for structure interrogation, based on a quantum mechanics database of  $^{13}\text{C}^\alpha$  chemical shifts. We report the application of *CheShift-2* to a local inconsistency between two X-ray crystal structures (PDB IDs 1IKN and 1NFI) of the complex between the p65/p50 heterodimer of NF $\kappa$ B and its inhibitor I $\kappa$ B $\alpha$ . The availability of NMR resonance assignments that included the region of the inconsistency provided an opportunity for independent validation of the *CheShift-2* server. Application of the server showed that the  $^{13}\text{C}^\alpha$  chemical shifts measured for the Gly270-Pro281 sequence close to the C-terminus of I $\kappa$ B $\alpha$  were unequivocally consistent with the backbone structure modeled in the

1IKN structure, and were inconsistent with the 1NFI structure. Previous NOE measurements had demonstrated that the position of a tryptophan ring in the region immediately N-terminal in this region was not consistent with either structure. Subsequent recalculation of the local structure in this region, based on the electron density of the deposited structure factors for 1IKN, confirmed that the local backbone structure was best modeled by 1IKN, but that the rotamer of Trp258 is consistent with the 1NFI structure, including the presence of a hydrogen bond between the ring N $\epsilon$ H of Trp258 and the backbone carbonyl group of Gln278. The consensus between all of these measures suggests that the *CheShift-2* server operates well under circumstances in which backbone chemical shifts are available but where local plasticity may render X-ray structural data ambiguous.

J. A. Vila · H. A. Scheraga  
Baker Laboratory of Chemistry and Chemical Biology,  
Cornell University, Ithaca, NY 14853-1301, USA

J. A. Vila  
IMASL-CONICET, Universidad Nacional de San Luis,  
Ejército de Los Andes, 950-5700 San Luis, Argentina

S.-C. Sue · H. J. Dyson (✉)  
Department of Molecular Biology, The Scripps Research  
Institute, 10550 North Torrey Pines Road, La Jolla,  
CA 92037, USA  
e-mail: dyson@scripps.edu

S.-C. Sue  
Department of Life Sciences, Institute of Bioinformatics  
and Structural Biology, National Tsing Hua University,  
Hsinchu, Taiwan

J. S. Fraser  
California Institute of Quantitative Biosciences (QB3)  
and Department of Cellular and Molecular Pharmacology,  
University of California, San Francisco, CA 94158, USA

**Keywords** Chemical shift · NF $\kappa$ B · I $\kappa$ B ·  
Structure validation

### Introduction

X-ray crystallography and NMR spectroscopy are the major techniques for determining the three-dimensional structures of proteins. One of the most challenging problems in NMR spectroscopy is the validation of the derived protein structures. Although a plethora of methods has been proposed to determine the accuracy and reliability of protein structures, there is consensus that more sophisticated structural validation methods are needed (Huang et al. 2005; Nabuurs et al. 2006; Bhattacharya et al. 2007; Vila and Scheraga 2009); the ideal validation tool would be a very sensitive, physics-based method to detect whether or not a given structure or regions of a structure, at the residue

level, is flawed. For this reason, we recently introduced *CheShift-2*, a fast and accurate algorithm for validating protein structures (Martin et al. 2012). This server exploits differences between observed and computed  $^{13}\text{C}^\alpha$  chemical shifts as a sensitive probe for possible local flaws in protein structures (Martin et al. 2012). However, differences between computed and observed  $^{13}\text{C}^\alpha$  chemical shifts are not always “flaws” and, hence, the origin of the discrepancies or inconsistencies must be investigated. This article reports the application of the *CheShift-2* server to a known problem, the distinction between local structures of the same protein that are locally inconsistent between two X-ray crystal structures.

The NF $\kappa$ B transcription factor family functions in the cell in response to external stimuli (Baeuerle 1998; Karin et al. 2002). The family consists of homodimers and heterodimers of five monomer units (p65, RelB, cRel, p50 and p52) each consisting of a pair of immunoglobulin-like domains (Baldwin 1996; Baeuerle and Baltimore 1996). The most common form of NF $\kappa$ B is a heterodimer of p65 and p50 (Sen and Baltimore 1986; Baldwin 1996). In resting cells, NF $\kappa$ B (p50/p65) is present in the cytoplasm as a complex with an inhibitor of the I $\kappa$ B family, most commonly I $\kappa$ B $\alpha$ , which contains an ankyrin domain of 6 repeats (Hayden and Ghosh 2004, 2008; shown schematically in Fig. 1a). The complex of NF $\kappa$ B (p50/p65) and I $\kappa$ B $\alpha$  has been characterized extensively, and X-ray structures of NF $\kappa$ B with I $\kappa$ B $\alpha$  (Jacobs and Harrison 1998; Huxford et al. 1998), as well as with DNA (Chen et al. 1998), are available. The X-ray structures of the NF $\kappa$ B-I $\kappa$ B $\alpha$  complex (Jacobs and Harrison 1998; Huxford et al. 1998) were published simultaneously from different research groups (Fig. 1b, c). Both structures showed the interaction of repeats 1–2 of I $\kappa$ B $\alpha$  with the C-terminal nuclear localization sequence (NLS) of p65 as well as intimate association between ankyrin repeats 4–6 and the dimerization domains of p50 and p65. Neither structure contained the DNA binding

domain of p50, and the DNA-binding domain of p65 was rotated from its position in the structure of NF $\kappa$ B (p50/p65) in complex with DNA (Chen et al. 1998). The sequence at the C-terminus of I $\kappa$ B $\alpha$ , immediately before a disordered PEST-like sequence (i.e., a sequence rich in Pro, Glu, Ser and Thr residues), showed the largest difference between the two X-ray structures. Indeed, the structure of this region differed not only in the length of the modeled sequence, but in the alignment of the structure with the amino acid sequence, although both structures showed this region located some 25–30 Å from the DNA-binding loops of the p65 DNA binding domain. The relatively long distance between the C-terminal region of I $\kappa$ B $\alpha$  and the DNA binding loops of NF $\kappa$ B was puzzling, because truncation of even a small portion of the C-terminal PEST sequence results in significantly weaker binding of I $\kappa$ B $\alpha$  to NF $\kappa$ B (Kumar and Gelinas 1993; Ernst et al. 1995; Bergqvist et al. 2008) and in loss of the ability of I $\kappa$ B $\alpha$  to strip NF $\kappa$ B from DNA (Bergqvist et al. 2009). Recent NMR experiments have established that the PEST sequence makes at least transient contact with the DNA binding loops of p65 and that the local backbone and side-chain conformation modeled for the C-terminal sequence of I $\kappa$ B $\alpha$  is not correct in either of the two X-ray structures (Sue and Dyson 2009). NOEs observed between the Trp N $\epsilon$ H and backbone amides in the PEST sequence established the fit of the backbone structure to the amino acid sequence and the correct conformation of the tryptophan ring (Sue and Dyson 2009). As part of this work, resonance assignments were made for the C-terminal region of I $\kappa$ B $\alpha$  in complex with p50(248–350)/p65(19–321). The present work describes the application of the *CheShift-2* server algorithm to these chemical shift data, with the aim of determining whether the server can decide on the basis of chemical shift data alone which crystallographic model is correct.

The physics-based approach of *CheShift-2* differs from knowledge-based methods [for example, those of Shen and

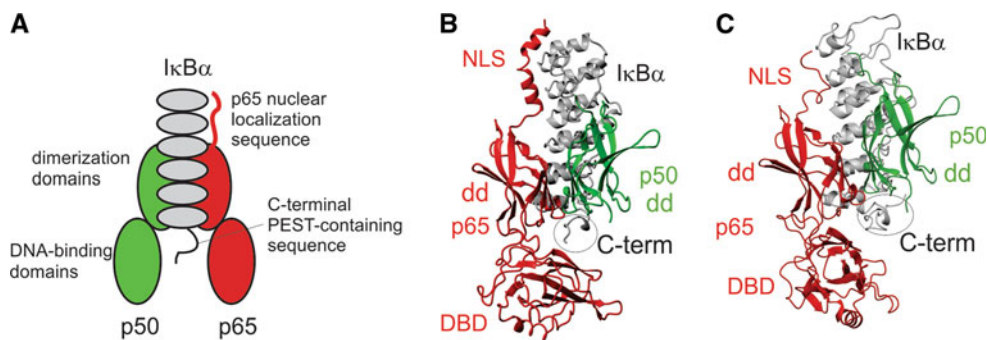


**Fig. 1** **A** Schematic diagram showing the NF $\kappa$ B heterodimer of p50 (green) and p65 (red) in complex with the ankyrin repeat domain of I $\kappa$ B $\alpha$  (gray). Both p50 and p65 consist of two immunoglobulin-like domains (shown as ellipses), an N-terminal DNA-binding domain and

a C-terminal dimerization domain. **B, C** Backbone ribbon showing the X-ray crystal structures of the NF $\kappa$ B (p65/p50)/I $\kappa$ B $\alpha$  complex. **B** 1NFI (Jacobs and Harrison 1998); **C** 1IKN (Huxford et al. 1998)

Bax (2007), Han et al. (2011)], which are able to predict the chemical shifts for several nuclei, not only for  $^{13}\text{C}^\alpha$ , as is done with *CheShift2*. It is beyond the scope of this work to compare the structure-validation capabilities of physics-based and knowledge-based methods.

## Results

The domain of human  $\text{I}\kappa\text{B}\alpha$  that interacts with the p65/p50 NF $\kappa\text{B}$  heterodimer consists of residues 67–317, and includes 6 ankyrin repeat domains and a C-terminal sequence (residues 281–317) rich in Ser, Pro, Glu and Thr residues (Fig. 2). The C-terminal sequence has been termed a “PEST” sequence, and it appears to be largely disordered in solution. Crystal structures of the complex between  $\text{I}\kappa\text{B}\alpha$  and p65/p50 NF $\kappa\text{B}$  (Jacobs and Harrison 1998; Huxford et al. 1998) were obtained with a construct of  $\text{I}\kappa\text{B}\alpha$  truncated at the C-terminus to contain residues 67–287, but neither of the structures was able to define the complete C-terminal sequence, due to crystallographic disorder. Coordinates were reported for residues Asp73-Ser293 (Huxford et al. 1998) and for residues Leu70-Glu282 (Jacobs and Harrison 1998). The NMR experiments (Sue and Dyson 2009) were performed with the same constructs as had been used in the crystallographic studies, and resonance assignments were obtained for all residues of  $\text{I}\kappa\text{B}\alpha$ , including the entire truncated “PEST” sequence up to residue 287 (Sue and Dyson 2009). For the purposes of the comparison reported in this work, only the  $\text{I}\kappa\text{B}\alpha$  assignments for residues 270–281 were used, representing the area of the structural discrepancy in the reported X-ray coordinates.

TROSY NMR spectra of the complex of  $\text{I}\kappa\text{B}\alpha$  (67–287) with deuterated NF $\kappa\text{B}$  p65(19–321)/p50(248–350) are well resolved despite their relatively high molecular weight (Fig. 3) and can be assigned with reference to complexes of smaller constructs of NF $\kappa\text{B}$  (Sue et al. 2008). Backbone  $^{13}\text{C}^\alpha$  chemical shifts for the  $\text{I}\kappa\text{B}\alpha$  sequence Gly270-Pro281,

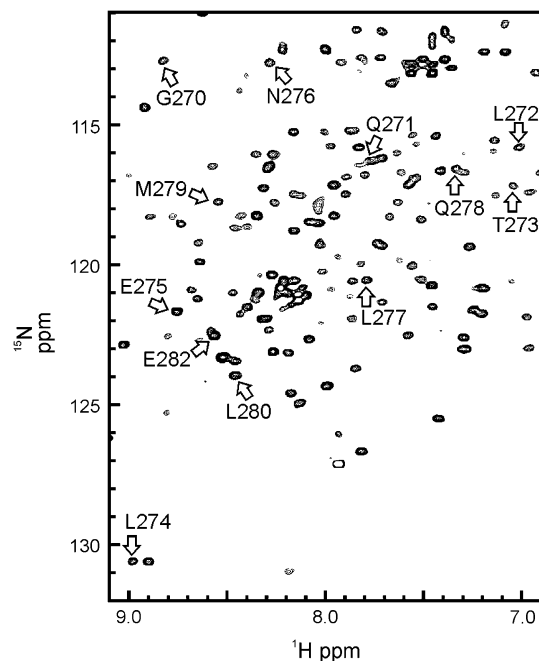


**Fig. 3** Portion of a 2D  $^1\text{H}$ - $^{15}\text{N}$  TROSY-HSQC spectrum of  $^{15}\text{N}$ -labeled  $\text{I}\kappa\text{B}\alpha$  (67–287) in complex with deuterated p65(19–321)/p50(248–350). Resonance assignments for the residues in Table 1 are shown [adapted from (Sue and Dyson 2009)]

together with the corresponding coordinates from the protein structures of 1NFI and 1IKN, respectively, were used as input in *CheShift-2*, and the results of the graphical validation are shown in Figs. 4a and 5a. The difference between the observed and computed  $^{13}\text{C}^\alpha$  chemical shifts for each residue is summarized in Table 1. This difference is clearly uniformly greater for the 1NFI crystal structure (Jacobs and Harrison 1998) (Fig. 4b) compared to the 1IKN structure (Huxford et al. 1998) (Fig. 5b). The results shown in Figs. 4 and 5 demonstrate that 1IKN is a better representation of the observed backbone chemical shifts in this region than 1NFI.

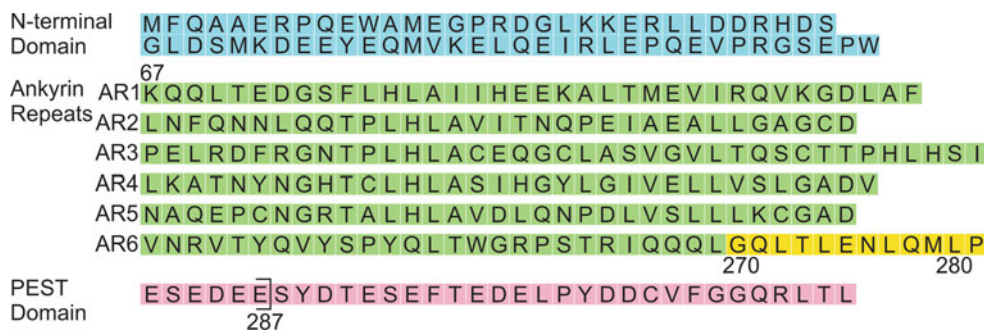


**Fig. 2** Amino acid sequence of human  $\text{I}\kappa\text{B}\alpha$  showing the various regions of the protein. The N-terminal domain (not examined in this work) is shown in blue, the ankyrin repeats in green and the C-terminal PEST-like sequence in pink, with the end of the 67–287

construct indicated by a bracket. The residues at the C-terminal end of AR6, for which the analysis was made with *CheShift-2* (Table 1) are shown in yellow

**Fig. 4** **A** Structure of the segment Gly270 to Pro281 of  $I\kappa B\alpha$ , derived from 1NFI (Jacobs and Harrison 1998) colored by *CheShift-2*, which discriminates small (*blue*), medium (*white*) and large (*red*) deviations from the structure expected on the basis of the chemical shifts. **B** Correlation of the observed chemical shifts (Sue and Dyson 2009) and those calculated from the 1NFI structure using *CheShift-2*

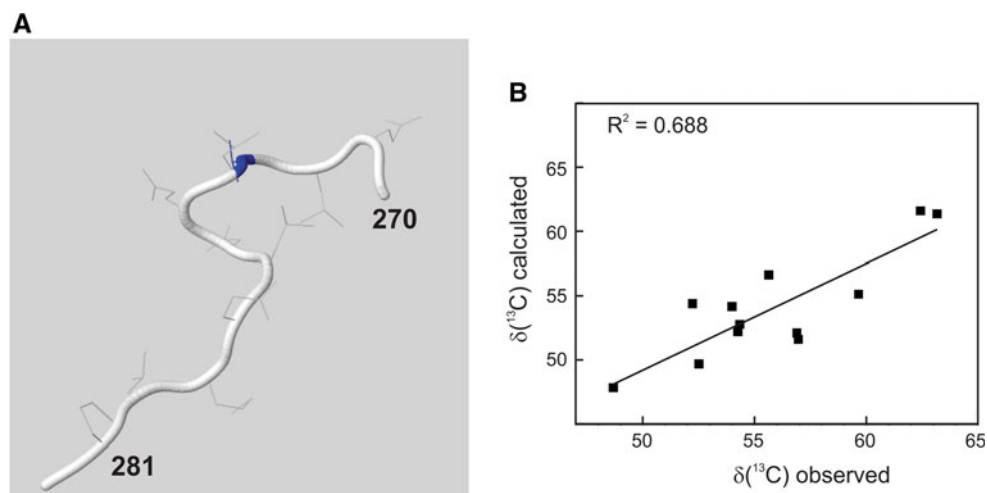


**Fig. 5** **A** Structure of the segment Gly270 to Pro281 of  $I\kappa B\alpha$ , derived from 1IKN (Huxford et al. 1998) colored by *CheShift-2*, which discriminates small (*blue*), medium (*white*) and large (*red*) deviations from the structure expected on the basis of the chemical shifts. **B** Correlation of the observed chemical shifts (Sue and Dyson 2009) and those calculated from the 1IKN structure using *CheShift-2*

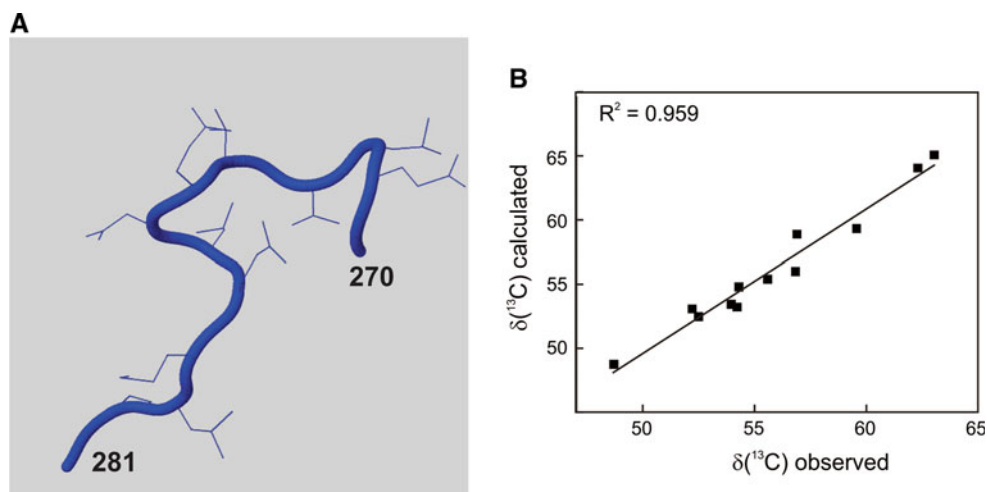


**Table 1** Differences between computed and observed  $^{13}\text{C}^\alpha$  chemical shift values for the segment Gly270 to Pro281 of proteins 1IKN and 1NFI, respectively

Sequence	$\langle \Delta\mu \rangle_{1\text{NFI}}$	$\langle \Delta\mu \rangle_{1\text{IKN}}$
Gly270	3.0	1.1
Gln271	2.5	0.9
Leu272	2.8	1.6
Thr273	1.4	1.0
Leu274	2.4	0.8
Glu275	1.9	0.1
Asn276	2.3	0.5
Leu277	2.4	0.7
Gln278	3.0	0.9
Met279	3.1	0.6
Leu280	1.8	1.0
Pro281	1.8	1.0

X-ray structure factors have been deposited in the Protein Data Bank for 1IKN (Huxford et al. 1998). Using these deposited structure factors, the electron density maps were recalculated. These maps were consistent with the backbone of 1IKN and thus with all of the experimental and theoretical data that have been accumulated on this sequence in the complex. In the recalculated structural model, the indole ring of Trp258 is oriented so that there is a hydrogen bond between its  $\text{N}\epsilon\text{H}$  and the backbone carbonyl group of Gln278, as inferred from the NMR NOE results (Sue and Dyson 2009), rather than the carbonyl group of Leu277 (Jacobs and Harrison 1998). The alignment of the backbone in the re-calculated model based on a reanalysis of the structure factors comfortably corresponds to that of 1IKN, with the Trp258 side chain conformation consistent with 1NFI and the NMR data. To further validate this new model, we examined the model calculated by PDB-REDO (Joosten et al. 2012), which uses automated

pipelines to re-refine datasets using modern software and makes these models publically accessible. The fully optimized PDB-REDO model also contains the Trp258 side chain orientation with the hydrogen bond to the Gln278 backbone. These results confirm that the *CheShift-2* server, using chemical shift data alone, validated the correct structural model in this case.

## Discussion

It is quite common for the N- and C-terminal residues of proteins to be disordered in crystal structures. Such regions are frequently omitted from structure models, or modeled with high temperature factors, which are often interpreted as evidence of disorder. Heterogeneity in the structures of loops and side chains has recently been exploited in room-temperature crystallography experiments to extract multiple structures (Fraser et al. 2009; Arnautova et al. 2009). The two structures of the NF $\kappa$ B-I $\kappa$ B $\alpha$  complex (Jacobs and Harrison 1998; Huxford et al. 1998) have reported models for the C-terminal region of I $\kappa$ B $\alpha$  that differ in length as well as in the alignment of the backbone structure to the amino acid sequence and local side-chain conformation. Such ambiguity is not unexpected, given the likelihood that the electron density in the region will be difficult to model due to flexibility. The NMR spectrum also indicates that the C-terminal portion of I $\kappa$ B $\alpha$  is flexible, with poor dispersion of amide proton chemical shifts and relatively strong cross peaks in the  $^1\text{H}$ - $^{15}\text{N}$  HSQC spectrum (Fig. 3).

The local structure in the C-terminal region of I $\kappa$ B $\alpha$  is of interest because biochemical evidence suggests that the PEST sequence makes contact with the DNA-binding loops of NF $\kappa$ B p65 (Ernst et al. 1995; Kumar and Gelinas 1993; Bergqvist et al. 2008), yet these regions are separated by >25 Å in both structures of the NF $\kappa$ B-I $\kappa$ B $\alpha$  complex (Jacobs and Harrison 1998; Huxford et al. 1998). It is likely that there is considerable crystallographic disorder in the C-terminal region of I $\kappa$ B $\alpha$ , which provides a possible rationale for reporting two different models for the same region. However, solution studies, including the NMR spectrum and the calculations derived from NMR data alone (without the necessity for a full 3D solution structure calculation) have allowed the local structure of this important region to be modified to give a result that not only reconciles the two published X-ray structures but also provides a satisfactory rationale for the biological observations (Sue and Dyson 2009). The system also provides a verifiable test of the applicability of the *CheShift-2* server for validation of local structures using only chemical shifts (Martin et al. 2012), information that is usually more readily available than NOEs and other less-sensitive NMR information such as coupling constants or relaxation data.

## Methods

Graphical visualization of the differences between observed and predicted  $^{13}\text{C}^\alpha$  chemical shifts (shown in Figs. 4a, 5a) was obtained by using the *CheShift-2* server (Martin et al. 2012) which made use of the following sequential steps: (1) for each amino acid residue  $\mu$ , the difference between observed (Obs) and predicted (Pred)  $^{13}\text{C}^\alpha$  chemical-shifts,  $\Delta_\mu = ({}^{13}\text{C}^\alpha, \text{Obs} - {}^{13}\text{C}^\alpha, \text{Pred})$ , is computed; (2) the  $\Delta_\mu$  value computed for each residue  $\mu$  is smoothed by averaging it over the values of the nearest-neighbor residues on each side; (3) the resulting averaged  $\langle \Delta_\mu \rangle$  value is discretized, i.e.,  $\langle \Delta_\mu \rangle_{\text{integer}}$  can adopt the values of 1, 0 or  $-1$ , depending on the magnitude of the average differences ( $\langle \Delta_\mu \rangle$ ), as explained below; and (4) these discretized values are mapped onto the 3D protein model and associated with a color, blue, white or red, respectively. Implicit in this color-code assignment is the assumption that average differences per residue between observed and predicted  $^{13}\text{C}^\alpha$  chemical shifts, which are within  $\sim 1.7$  ppm (blue), are considered as small; within  $\sim 3.4$  ppm (white) they are considered as medium, an indication of possible inconsistencies in the experimental data; beyond 3.4 ppm (red), they are considered as large differences and, hence, special attention should be paid to those residues.

Electron density maps based on the structure factors for 1IKN were calculated using Phenix (Adams et al. 2010) and analyzed using Coot (Emsley et al. 2010). The fully optimized PDB\_REDO model was retrieved from the public PDB\_REDO website: ([http://www.cmbi.ru.nl/pdb\\_redo/ik/1ikn/index.html](http://www.cmbi.ru.nl/pdb_redo/ik/1ikn/index.html)).

**Acknowledgments** This work was supported by grants GM71862 (HJD), DP5OD009180 (JSF), GM14312 (HAS) from the National Institutes of Health and PIP-112-2011-0100030 (JAV) from IMASL-CONICET, Argentina.

## References

- Adams PD, Afonine PV, Bunkoczi G, Chen VB, Davis IW, Echols N, Headd JJ, Hung LW, Kapral GJ, Grosse-Kunstleve RW, McCoy AJ, Moriarty NW, Oeffner R, Read RJ, Richardson DC, Richardson JS, Terwilliger TC, Zwart PH (2010) PHENIX: a comprehensive Python-based system for macromolecular structure solution. *Acta Crystallogr D* 66:213–221
- Arnaudova YA, Vila JA, Martin OA, Scheraga HA (2009) What can we learn by computing  $^{13}\text{C}$  chemical shifts for X-ray protein models? *Acta Crystallogr D* 65:697–703
- Baeuerle PA (1998) I $\kappa$ B-NF- $\kappa$ B structures: at the interface of inflammation control. *Cell* 95:729–731
- Baeuerle PA, Baltimore D (1996) NF- $\kappa$ B: ten years after. *Cell* 87:13–20
- Baldwin AS (1996) The NF- $\kappa$ B and I- $\kappa$ B proteins: new discoveries and insights. *Ann Rev Immunol* 14:649–683

- Bergqvist S, Ghosh G, Komives EA (2008) The I $\kappa$ B $\alpha$ /NF- $\kappa$ B complex has two hot spots, one at either end of the interface. *Protein Sci* 17:2051–2058
- Bergqvist S, Alverdi V, Mengel B, Hoffmann A, Ghosh G, Komives EA (2009) Kinetic enhancement of NF- $\kappa$ B-DNA dissociation by I $\kappa$ B $\alpha$ . *Proc Natl Acad Sci USA* 106:19328–19333
- Bhattacharya A, Tejero R, Montelione GT (2007) Evaluating protein structures determined by structural genomics consortia. *Proteins* 66:778–795
- Chen FE, Huang DB, Chen YQ, Ghosh G (1998) Crystal structure of p50/p65 heterodimer of transcription factor NF- $\kappa$ B bound to DNA. *Nature* 391:410–413
- Emsley P, Lohkamp B, Scott WG, Cowtan K (2010) Features and development of coot. *Acta Crystallogr D Biol Crystallogr* 66:486–501
- Ernst MK, Dunn LL, Rice NR (1995) The PEST-like sequence of I $\kappa$ B $\alpha$  is responsible for inhibition of DNA binding but not for cytoplasmic retention of c-Rel or RelA homodimers. *Mol Cell Biol* 15:872–882
- Fraser JS, Clarkson MW, Degnan SC, Erion R, Kern D, Alber T (2009) Hidden alternative structures of proline isomerase essential for catalysis. *Nature* 462:669–673
- Han B, Liu Y, Ginzinger SW, Wishart DS (2011) SHIFTX2: significantly improved protein chemical shift prediction. *J Biomol NMR* 50:43–57
- Hayden MS, Ghosh S (2004) Signaling to NF- $\kappa$ B. *Genes Dev* 18:2195–2224
- Hayden MS, Ghosh S (2008) Shared principles in NF- $\kappa$ B signaling. *Cell* 132:344–362
- Huang YJ, Powers R, Montelione GT (2005) Protein NMR recall, precision, and F-measure scores (RPF scores): structure quality assessment measures based on information retrieval statistics. *J Am Chem Soc* 127:1665–1674
- Huxford T, Huang DB, Malek S, Ghosh G (1998) The crystal structure of the I $\kappa$ B $\alpha$ /NF- $\kappa$ B complex reveals mechanisms of NF- $\kappa$ B inactivation. *Cell* 95:759–770
- Jacobs MD, Harrison SC (1998) Structure of an I $\kappa$ B $\alpha$ /NF- $\kappa$ B complex. *Cell* 95:749–758
- Joosten RP, Joosten K, Murshudov GN, Perrakis A (2012) PDB\_REDO: constructive validation, more than just looking for errors. *Acta Crystallogr D Biol Crystallogr* 68:484–496
- Karin M, Cao Y, Greten FR, Li ZW (2002) NF- $\kappa$ B in cancer: from innocent bystander to major culprit. *Nat Rev Cancer* 2:301–310
- Kumar S, Gelinas C (1993) I $\kappa$ B $\alpha$ -mediated inhibition of  $\nu$ -Rel DNA binding requires direct interaction with the RXXRXXRXXC Rel/ $\kappa$ B DNA-binding motif. *Proc Natl Acad Sci USA* 90:8962–8966
- Martin OA, Vila JA, Scheraga HA (2012) CheShift-2: graphic validation of protein structures. *Bioinformatics* 28:1538–1539
- Nabuurs SB, Spronk CAEM, Vuister GW, Vriend G (2006) Traditional biomolecular structure determination by NMR spectroscopy allows for major errors. *PLoS Comput Biol* 2:71–79
- Sen R, Baltimore D (1986) Inducibility of  $\kappa$  immunoglobulin enhancer-binding protein NF- $\kappa$ B by a posttranslational mechanism. *Cell* 47:921–928
- Shen Y, Bax A (2007) Protein backbone chemical shifts predicted from searching a database for torsion angle and sequence homology. *J Biomol NMR* 38:289–302
- Sue SC, Dyson HJ (2009) Interaction of the I $\kappa$ B $\alpha$  C-terminal PEST sequence with NF- $\kappa$ B: insights into the inhibition of NF- $\kappa$ B DNA binding by I $\kappa$ B $\alpha$ . *J Mol Biol* 388:824–838
- Sue SC, Cervantes C, Komives EA, Dyson HJ (2008) Transfer of flexibility between ankyrin repeats in I $\kappa$ B $\alpha$  upon formation of the NF- $\kappa$ B complex. *J Mol Biol* 380:917–931
- Vila JA, Scheraga HA (2009) Assessing the accuracy of protein structures by quantum mechanical computations of <sup>13</sup>C(alpha) chemical shifts. *Acc Chem Res* 42:1545–1553